Organocatalyzed ring opening polymerization of lactide from the surface of cellulose nanofibrils

Michael Lalanne-Tisné, Maarten A. Mees, Samuel Eyley, Philippe Zinck, Wim Thielemans

Organocatalyzed ring opening polymerization of lactide from the surface of cellulose nanofibrils

Michael Lalanne-Tisné[1,2], Maarten A. Mees[1], Samuel Eyley[1], Philippe Zinck[2*], Wim Thielemans[1*]

[1] Sustainable Materials Lab, Department of Chemical Engineering, KU Leuven, campus Kulak Kortrijk, Etienne Sabbelaan 53, box 7659, B-8500 Kortrijk, Belgium

*wim.thielemans@kuleuven.be

[2] Université de Lille, CNRS, Centrale Lille, ENSCL, Univ. Artois, UMR 8181 - UCCS - Unité de Catalyse et Chimie du Solide, F-59000 Lille, France

*philippe.zinck@univ-lille.fr

Abstract:

The surface initiated ring opening polymerization (SI-ROP) of cellulose nanofibers (CNF) with *rac*-Lactide under mild conditions using N,N-dimethyl aminopyridine (DMAP) was investigated. The influence of catalyst amount, monomer-to-initiator (cellulose surface –OH groups) ratio, temperature, and cellulose preconditioning (lyophilization *vs* solvent exchange) were studied to determine the best SI-ROP conditions, and to understand the effect of the parameters on grafting efficiency. The fibers modified after lyophilization had a PLA content comparable to those obtained with traditional metal catalysts (e.g. tin-(II)ethylhexanoate). Starting from a stable dispersion of CNF in dichloromethane obtained through solvent-exchange showed better results at low catalyst amounts. Furthermore, DMAP was readily removed from the products whereas metal catalysts can be hard to remove from the final material, potentially shortening the material lifespan and making it unfit for some applications. Therefore, the use of an easily removable and more efficient organocatalyst can be considered a good alternative to metal catalysts.

Keywords:

Cellulose nanofibrils, Organocatalysis, Polylactide, Biocomposite

1. Introduction

After playing an important role in the advent of the chemical industry and being replaced by petroleum-based alternatives, carbohydrate polymers have again regained an increasing amount of attention. Polysaccharides have been the focus of a large amount of work as the biggest fraction of renewable biomass, with cellulose being the most common biopolymer on the planet with an estimated annual production of well over 10^{10} tons (Habibi, Lucia, & Rojas, 2010). Cellulose has many potential uses, and can be made into nanomaterials such as cellulose nanofibrils (CNF) (Siqueira, Bras, & Dufresne, 2010; Zhao, Du, Chen W., Pan, & Chen D., 2019) and cellulose nanocrystals (Habibi et al., 2010; Zhao et al., 2019). CNF are micron-length fibers that possess remarkable properties such as a high aspect ratio (width of 4 to 20 nm, length of up to several microns), a high stiffness with a Young's modulus superior to 110 GPa, and a low density of 1.6 g/cm^3 (Dufresne, 2013), capable of forming a network structure. Unlike CNFs, CNCs do not contain dislocated non-crystalline sections as the dislocated regions are removed during an acid hydrolysis, making their length smaller and crystallinity higher (Bondeson, Mathew, & Oksman, 2006)**Erreur ! Source du renvoi introuvable.**. Their high abundance, stiffness, and high aspect ratio make CNFs and cellulose nanocrystals (CNCs) good candidates for use in composite materials as reinforcements (Eichhorn et al., 2010). Moreover, nanocellulose can be produced at an industrial scale (Liu, Moon, Rudie, &

Youngblood, 2014; Trache, Hussin, Haafiz, & Thakur, 2017). Because of the lower aspect ratio of CNCs when compared to CNFs, CNFs have a greater potential as reinforcing fiber and impact modifier in composites (Xu et al., 2013), yet they have not received the same amount of attention as CNCs when it comes to surface modification (Xie, Du, Yang, & Si, 2018). Using CNFs and CNCs in polymer matrices comes with a few challenges; the compatibility between hydrophobic polymer matrices and hydrophilic cellulose is limited, and the dispersion of nanomaterials in polymer can be quite poor. This in turn diminishes the achievable mechanical strength and ductility improvements of the composite material as these depend on individualization of the reinforcing fibers. Hence, some research has been carried out on the surface modification of nanocellulose to enhance their dispersibility and to improve the compatibility of cellulose nanomaterials with hydrophobic polymer matrices. Their surface hydroxyl groups allow for a wide array of chemical modifications and these could thus be used to change the nanocellulose surface energy to increase compatibility with polymer matrices (Eyley & Thielemans, 2014; Habibi, 2014). Examples of modifications reported in the literature include non-covalent modification such as surfactant adsorption (Bondeson & Oksman, 2007; Heux, Chauve, & Bonini, 2000), but also covalent surface reactions such as sulfonation (Abitbol, Kloser, & Gray, 2013; Liimatainen, Visanko, Sirviö, Hormi, & Niinimaäki ,2013), oxidation (de Nooy, Besemer, & van Bekkum 2010; Isogai, Saito, & Fukuzumi, 2011), acetylation (Yamamoto, Horii, & Hirai, 2006; Yang et al., 2013), etherification (Hasani, Westman, & Gray, 2008), silylation (Goussé, Chanzy, Excoffier, Soubeyrand, & Fleury, 2002), and amidation (Lasseuguette, 2008).

The combination of a biodegradable, biocompatible, and bio-based polymer with CNFs could lead to an all-biodegradable and biocompatible composite material made completely from renewable materials. Polylactide (PLA), a polyester that can be obtained from 100% renewable sources, is therefore an interesting candidate (Drumright, Gruber & Henton, 2000). In addition, PLA is non-toxic and biocompatible, allowing it to be used in many fields such as food-contact and biomedical application (Munim & Raza, 2019). Combining cellulose fibers with PLA could thus lead to materials with a larger range of mechanical and impact properties opening up a wider range of possible applications than those now achievable (Avinc & Khoddami, 2009). Using the same monomer to graft on the cellulose as the polymer matrix should provide the best possible compatibility between matrix and reinforcing fiber (Nordgren, Lönnberg, Hult, Malmström, & Rutland, 2009). Surface modification of CNF with polymers could also be useful for the production of co-continuous composites, where the polymeric surface graft acts as the complete matrix phase with near-perfect compatibility between the matrix and the fiber (Labet, Thielemans & Dufresne, 2007).

Cellulose and other polysaccharides with PLA grafts have mostly been reported using a "grafting from" approach (Gazzotti et al., 2019; Stepanova et al., 2019; Ouchi, Kontani, & Ohya, 2003; Miao, Rousseau, Mortreux, Martin, & Zinck, 2011), but "grafting to" methods have also been used successfully to produce similar materials (Ohkita & Lee, 2004). In the case of lactide and other similar cyclic monomers, the grafting from approach makes use of ring-opening polymerization (ROP), using the polysaccharide hydroxyl groups as initiating sites along with a catalyst, often tin(II) octoate ($SnOct_2$) (Gazzotti et al., 2019) or DMAP (Miao et al., 2011; Ohkita & Lee, 2004). ROP reactions from nanocellulose have been performed in solution and in bulk under a wide variety of condition (Labet & Thielemans, 2012; Ohkita & Lee, 2004). A previous report of PLA-grafted cellulose nanofibrils using the "grafting from" approach and $SnOct_2$ achieved a grafting of around 20w% of PLA (Stepanova et al. 2019).

Metal-based catalysts, and in particular tin, have been used for a long time to perform ring-opening polymerization of lactides, both for homogeneous PLA synthesis and for the grafting from carbohydrates as described previously. However, metal catalysts can cause problems as they are prone to stay attached to the chain end of the macromolecular product (Hafrén & Córdova, 2005), requiring additional steps for removal implying an increased cost for sensitive applications such as biomedical applications. Even these steps in general do not fully remove the metal catalysts in the presence of cellulose, making trace pollution a potential problem (Labet 2012).

Organic catalysis is an interesting alternative to metal-based catalysis and it has been heavily investigated in the last few decades for the ROP of lactide (Dove, 2012; Kiesewetter, Shin, Hedrick, & Waymouth, 2010; Ottou, Sardon, Mecerreyes, Vignolle, & Taton, 2016). A wide range of organocatalysts can be used including N-heterocylic carbenes (Li, Ai, & Hong, 2018), pyridine-based compounds (Miao et al., 2011; Ohkita & Lee, 2004), guanidine (Lohmeijer et al., 2006; Simón & Goodman, 2007) , amidine (Simón & Goodman, 2007), and nucleobases such as adenine (Nogueira et al., 2016). Most of these have received thorough studies for the ROP of lactide and were proven to be competitive with metal-based catalysts.

While both ROP of lactide initiated from polysaccharide hydroxyl groups and catalyzed by an organocatalyst have been studied, the SI-ROP of PLA from nanocelluloses catalyzed by an organic compound has not received such attention. In addition, the surface modification of cellulose nanocrystals has been reported more often than surface modification on nanofibrils, with little work done on studying the influence of different parameters on the reaction of polymerization initiated from nanocellulose surfaces. Where such studies have been carried out, they proved to be quite valuable in bringing insights in the reaction of SI-ROP and enabled optimization of the modification reaction (Labet & Thielemans, 2012). Furthermore, while formation of homopolymer is also expected as trace water cannot be fully excluded from the reaction mixture, little is known about the competition between homopolymerization and

polymerization from the nanocellulose surface. We report herein an investigation of the influence of experimental parameters on the grafting efficiency of lactides in the DMAP catalyzed CNF hydroxyl groups initiated ROP reaction to start developing the insights needed to optimize these reactions.

2. Materials and Methods

2.1. Material

Cellulose nanofibrils were obtained from SAPPI and received as a 1% suspension in water and was used as the initiator for the reaction, and the main material used in this study. This product is available commercially under the brand name Valida. Characterization data of non-modified cellulose is provided in Supplementary Information. Dichloromethane (analytical reagent grade) was obtained from Van Waters Rogers (VWR) and used as both the reaction solvent and for purification, acetone and ethanol were purchased from Acros Organics and were used for purification. *Rac*-Lactide was used as the monomer and received from Fisher Scientific and N,N-dimethyl aminopyridine was use as catalyst of the reaction and received from Sigma Aldrich. All chemicals except for cellulose were used as received.

2.2. Surface-Initiated Ring Opening Polymerization (SI-ROP)

- SI-ROP from lyophilized cellulose nanofibrils

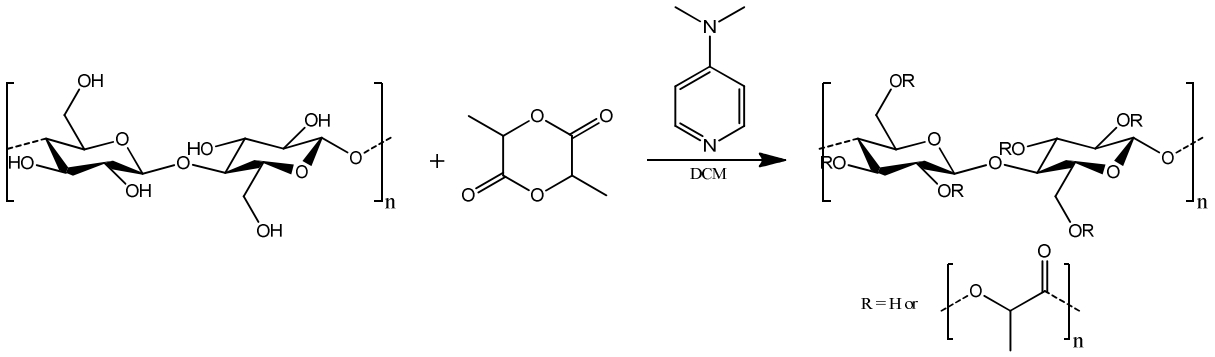

Figure 1: Reaction scheme of the Surface-Initiated Ring-Opening Polymerization (SI-ROP) of DL-Lactide from the surface of cellulose nanofibrils using N,N-dimethyl aminopyridine (DMAP) as catalyst dichloromethane (DCM) as the solvent

CNFs were first frozen using liquid nitrogen, and then freeze-dried for 4 days at -56°C with a Thermo Heto PowerDry PL6000, under a vacuum of 2 mbar. After lyophilization, the CNFs were soxhlet-extracted with ethanol for 24 hours to remove any impurities adsorbed on the surface of the cellulose fibers (Labet & Thielemans, 2011). The CNFs were subsequently dried at 40°C for 24h, under vacuum at around 3 mbar.

Surface modification of the freeze-dried CNFs was performed in a 100 mL 3-necked round bottom flask under an inert atmosphere (argon) while stirring continuously. First CNF and lactide were introduced in the flask, placed under vacuum, and flushed with argon for 15 minutes. Then dichloromethane (DCM) was added and the mixture was left to stir for another 15 minutes. Finally, DMAP was introduced and the mixture was heated to 35°C. A condenser was connected to the round bottom flask to avoid gas build-up and pressure increase in the flask. After 48 hours, the reaction mixture was filtered over a cellulose soxhlet extraction thimble and purified by soxhlet extraction with dichloromethane for 24 hours to remove homopolymer. An additional soxhlet extraction with ethanol was performed for 24 hours to remove DMAP from the surface of cellulose. The modified nanofibrils were subsequently dried *in vacuo* for 24 hours at 40°C and a pressure of 3 mbar. The reaction scheme for SI-ROP is presented in Figure 1.
For all those reactions, the temperature was set to 35°C for all reactions, and the monomer/cellulose ratio was set at 30/1, while the catalyst loading was gradually increased from 0.5eq to 5eq.

- SI-ROP from never-dried CNF dispersion

A known amount of 1 wt% CNF/H_2O dispersion was poured in a 1L round bottom flask and mixed with an equal part of ethanol. The resulting suspension was filtered through a large cellulose soxhlet extraction thimble and purified by soxhlet extraction with acetone (8h) to remove water from the cellulose. The CNF were then further purified by soxhlet extraction with ethanol (24h) and then with DCM (6,5h). Care was taken to always keep the CNF in the extraction thimble in a wet state to avoid drying-induced aggregation. The cellulose obtained was then mixed with additional DCM to obtain a 1% suspension of CNF in DCM. Surface modification of cellulose was performed in a 100 mL 3-necked round bottom flask under inert atmosphere (argon) while stirring continuously. DMAP was first introduced in the flask connected to a condenser and flushed with argon for 15 minutes. Ten mL of the cellulose dispersion in DCM was then added and stirred with DMAP to allow it to adsorb to the surface of cellulose. Five mL of pure dichloromethane was then added to the mixture, followed by lactide. The reaction was subsequently heated to the desired reaction temperature and stopped after 24 hours. The mixture was first filtered through a cellulose soxhlet extraction thimble and then purified by DCM soxhlet extraction for 24h to remove homopolymer formed during the reaction. Another 24 hours, an ethanol soxhlet extraction was then carried out to clean cellulose of all the impurities still on its surface, especially DMAP. Finally, the solid was dried *in vacuo* at 40°C and a pressure of 3 mbar for 24 hours.

During all these experiments, the temperature was tested between 25°C and 39°C, the monomer/cellulose ratio was in a range between 1/1 to 30/1, and the catalyst loading was in a range of 0.5eq to 3eq.

2.3. Characterization

Elemental composition (C, H, N, and S) of CNFs was measured with a Thermo Scientific FLASH 2000 elemental analyzer (EA), using about 1 mg of dry sample. The standard used for calibration was 2,5-Bis(5-tert-butyl-2-benzo-oxazol-2-yl)thiophene (BBOT, Elemental Microanalysis, UK. Vanadium pentoxide was used to aid sulphur determination. All values reported are the average of 3 measurements.

Grafting percentage is evaluated by using the mass fraction of different elements in each sample, and then comparing the elemental composition with unmodified CNF and lactide. Water content, determined by TGA, is taken into account for the mass fraction of O and H for every measurement. The difference for each element mass fraction between the modified and unmodified cellulose is then used to determine what is the contribution of the grafts, which leads to the mass % of grafting done on CNFs. Unmodified CNF composition used for this calculus is provided by elemental analysis of the starting product, while lactide composition is assumed to be similar to its chemical formula.

A Netzsch TG 209 F3 Tarsus was used to carry out thermogravimetric analysis (TGA). Around 2 mg was placed in an aluminum-(III)-oxide pan and heated from 30 to 600°C at a ramp rate of 10°C/min under argon flow. Water content of the various samples was determined as the difference between the initial mass and the stabilized mass around 100°C. The determined water content was taken into account in the determination of the level of surface modification based on elemental composition results in line with our earlier reported procedure (Eyley et al. 2018).

Infrared spectra of CNF were measured using a Bruker ALPHA Fourier-transform Infrared Spectroscopy (FTIR) spectrophotometer to determine the success of the reaction on the CNF. Measurements were carried out in attenuated total reflection (ATR) mode. Spectra were acquired as the sum of 16 scans over a frequency ranging from 4000 to 400 cm^{-1} on CNF deposited onto the spectrophotometer.

Surface-sensitive analysis of modified CNF was carried out by X-ray photoelectron spectroscopy (XPS) on a Kratos Axis Supra photoelectron spectrometer using a monochromated Al Kα ($h\nu$ = 1486.7 eV, 5 mA) X-ray source, hybrid (magnetic/electrostatic) optics, and a hemispherical analyzer with a pass energy of 160 eV for survey spectra and 20 eV for high resolution spectra. Spectra were acquired under charge neutralization conditions using an electron flood gun within the field of the magnetic lens, and were charge corrected to aliphatic carbon at 285.0 eV. Spectra were processed in CasaXPS with Tougaard 2-parameter backgrounds used for integration and LA(α, m) lineshapes corresponding with a Voigtian function with Lorentzian exponent α and Gaussian width m used for fitting high resolution spectra. Empirical relative sensitivity factors supplied by Kratos Analytical (Manchester, UK) were used for quantification.

The crude homopolymer was extracted from dichloromethane soxhlet by removing the solvent using a rotary evaporator, and placing the product obtained in a vacuum oven at 40°C for 24h. The number-average molecular weight (Mn) and the dispersity (Đ) of the crude product were determined by Size Exclusion Chromatography (SEC) in tetrahydrofuran at 40 °C at a flow rate of 1 $mL.min^{-1}$. Sample concentration was of 2g/l, Mn and Đ were determined from the Refractive Index (RI) signal using a calibration curve based on polystyrene (PS) standards from Polymer Standards Service, on a Waters apparatus equipped with Waters Styragel columns HR2, HR3, HR5 and HR5E.

NMR was also used on some crude product extracted similarly to the one used for SEC analysis to characterize the homopolymer formed and evaluate the presence or not of unreacted monomer. ^{1}H NMR spectra were recorded on AVANCE III HD 300 Bruker spectrometer (7.1 Tesla) at room temperature in deuterated dimethyl sulfoxide (0.6 ml) for the crude mixture, as well as DMAP and DL-Lactide separately.

3. Results and discussion:

3.1. SI-ROP modification of lyophilized CNF

The effect of reaction temperature, catalyst loading, and monomer-to-cellulose ratio on the SI-ROP of PLA from the surface of freeze-dried CNF was investigated in order to optimize and control CNF functionalization. The reactions were first carried out in DCM using DMAP as the catalyst for 48h at 32°C. Representative examples of the reactant ratios and % of grafted PLA are given in Table 1.

At a fixed temperature and reaction time (35°C and 48 hours), the PLA content of grafted nanocellulose increased with the amount of catalyst, and reached a maximum for 3 equivalents of catalyst per surface hydroxyl group (Table 1).

Table 1: Evolution of grafted poly(lactide) content on the surface of cellulose using rac-Lactide, N,N-dimethyl aminopyridine (DMAP) as catalyst, lyophilized cellulose nanofibrils (CNF), in dichloromethane. Determined by elemental analysis (EA), calculation based on hydrogen and carbon content, corrected for water content.

Entry	T (°C)	Lactide/CNF	Eq DMAP/CNF	Grafted PLA (wt%)
1	35	30	0.5	6
2	35	30	1	6
3	35	30	1.5	8
4	35	30	2.0	8
5	35	30	2.5	11
6	35	30	3.0	19

7	35	30	4	12
8	35	30	5	17

Water present during the reaction competes with cellulose nanofibrils surface hydroxyl groups to initiate the polymerization reaction (Figure 1), thus resulting in homopolymer formation. This side reaction is important due to the hydrophilic nature of cellulose. It is further exemplified at DMAP amounts above 3 equivalents of the surface hydroxyl groups, where the grafted PLA content on the CNF dropped, indicating

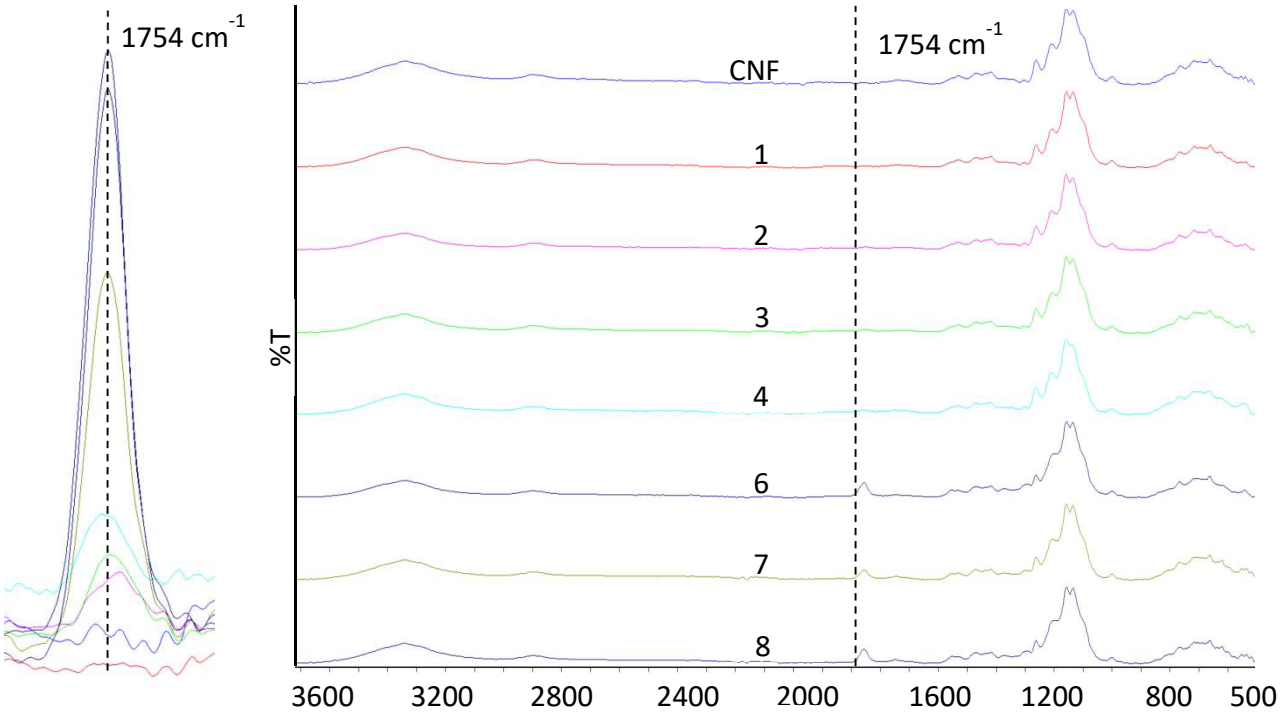

Figure 2: FT-IR spectra of cellulose nanofibrils (CNF) and modified CNF with different amount of grafting after purification by soxhlet extraction

that a higher catalyst amount leads to a faster initiation by water. Therefore a ratio [CNF]:[DMAP] of 3 appears to be optimal for CNF surface modification. This catalytic ratio is in the range of values reported in the literature for DMAP-catalyzed homopolymerization of lactide and for the ROP of lactide from polysaccharides (Miao et al., 2011; Nederberg, Connor, Möller, Glauser, & Hedrick, 2001; Siqueira et al., 2010).

In addition to elemental analysis, success of modification was confirmed by FTIR (Figure 2). The spectra of the product closely resembled that of cellulose as expected. The appearance of a band at 1754 cm^{-1} is characteristic of polylactide stretching frequencies for ν(C=O) and confirms successful esterification on the CNF surface, as well as a signal at 1451 cm^{-1} and 1090 cm^{-1}, which are typical for PLA (Miao et al., 2011; Nogueira et al., 2016). As shown in the magnification in Figure 2, the relative intensity of the carbonyl signal in modified CNF increased with increasing amount of catalyst, reaching a maximum for 3 equivalent

of catalyst/surface hydroxyl, in line with the trend observed for the calculated amount of PLA obtained from EA. This confirms the trend in surface modification and the maximum amount of PLA grafted on the

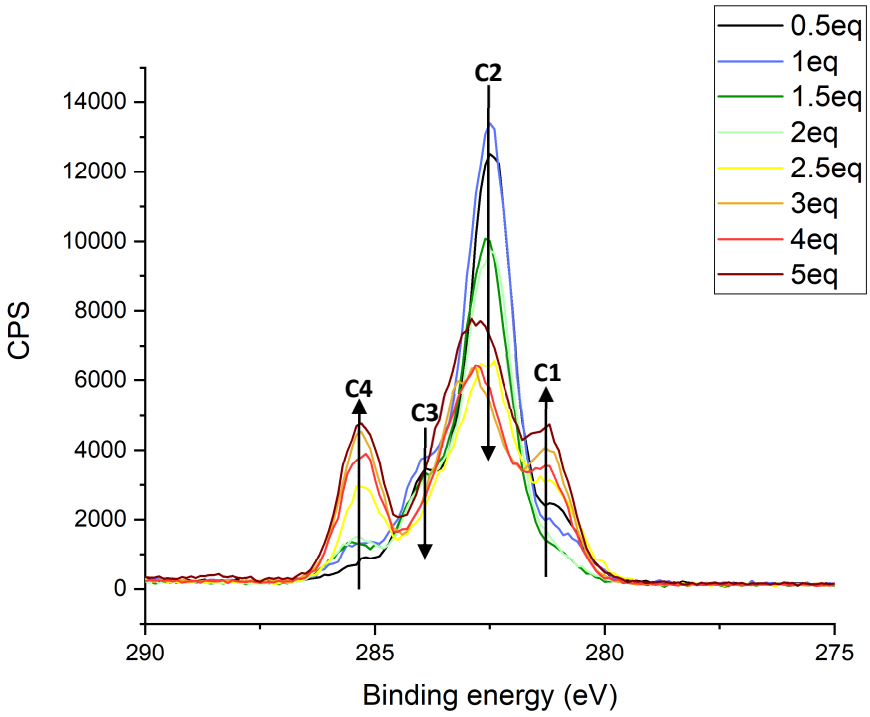

Figure 3: Carbon 1s X-ray Photoelectron Spectroscopy (XPS) scan of modified cellulose nanofibrils using different amounts of N,N-dimethyl aminopyridine

surface of cellulose for 3 equivalents of catalyst.

X-ray Photoelectron Spectroscopy (XPS) gives even more information on the surface composition and the chemical environment of the CNFs. In Figure 3, C1 is the aliphatic carbon contribution at 285eV, which initially increases with the amount of catalyst used. C2 and C3 correspond to C-O (at 286.41eV) and O-C-O (287.45eV) contribution respectively and both decreased with an increasing amount of PLA grafted on the surface of cellulose. C4 is the O-C=O contribution visible at 289.16eV, which increased with the amount of modification on the fiber in agreement with C1. Both C4 and C1 are not present for unmodified cellulose, confirming modification after purification of the CNF. All the positions reported for the different contributions are in agreement with earlier reported results for poly(ε-caprolactone) grafted on nanocellulose (Labet & Thielemans, 2011). XPS data thus confirmed the results obtained by elemental analysis and FTIR, with the most amount of modification detected for 3 equivalents of catalyst.

3.2. SI-ROP modification on never dried CNF

Using the results obtained from the previous experiments, a different protocol was tested using never-dried CNF. Indeed, working with lyophilized CNF requires freeze-drying, giving CNF that are more difficult to redisperse and that require the use of more solvent than never-dried CNF suspensions to obtain a homogeneous reaction mixture. Therefore, different methods for preparing CNF dispersions in DCM, from a water 1% water dispersion, were tested. We optimized the procedure and came to the methodology as described in the Materials and Methods section. The results of the DMAP-catalyzed ROP grafting reactions are reported in Table 2. This method gave a product that was easier to characterize after drying (powder-like) and showed in general a superior quantity of PLA grafting on CNF, particularly at lower amounts of catalyst (*e.g.* compare entries 3 and 4 in Table 1 to entry 10 in Table 2).

Using a ratio of lactide/CNF/catalyst of 30/1/3, two similar reactions were performed at 39°C over 24h, one using freeze-dried CNF and the other never-dried CNF. After using elemental analysis and TGA, the grafting obtained from freeze-dried cellulose was 13% (entry 16, table 2), while never dried cellulose grafting reached 24% (entry 15, table 2). As the result found for never-dried cellulose was comparable to better grafting obtained using freeze-dried cellulose over 48h, experiments using never-dried cellulose were performed over 24h Using never-dried CNF suspensions in DCM, we also investigated the effect of temperature, monomer amount, and monomer/initiator ratio.

Table 2: Evolution of grafted poly(lactide) content on the surface of cellulose using rac-lactide, N,N-dimethyl aminopyridine (DMAP) as catalyst and 0.1g cellulose nanofibrils dispersed in dichloromethane. Reaction time 24h. Determined by elemental analysis, calculation based on hydrogen and carbon content. Corrected for water content. a: done using freeze-dried CNF

Entry	T (°C)	Lactide/CNF	Eq DMAP/CNF	Grafted PLA (wt%)
1	25	1	0.5	7
2	25	1	3	13
3	25	15	1.75	7
4	25	30	0.5	16
5	25	30	3	18
6	32	1	1.75	5
7	32	15	0.5	9
8	32	15	1.75	11
9	32	15	3	9
10	32	30	1.75	12
11	39	1	0.5	6
12	39	1	3	17
13	39	15	1.75	12
14	39	30	0.5	18
15	39	30	3	24
16[a]	39	30	3	13

Grafting onto CNF ranged from 5% to 24%: Overall an increase in catalyst ratio from 0.5 eq to 3 eq led to an increase in the amount of PLA grafted onto CNF, irrespective of the temperature (comparing entry 1 to 2 and 12 to 11) or the quantity of lactide (comparing entry 1 to 2 and 5 to 4). As described previously, the polymerization reaction from the surface of CNF takes place in competition with the homopolymerization initiated by residual water. While DMAP is known to work better at higher quantities for ROP initiated by hydroxyl groups (Nederberg et al., 2001), the presence of a small amount of water means more catalyst is needed to ensure a proper initiation from the nanofibril surface.

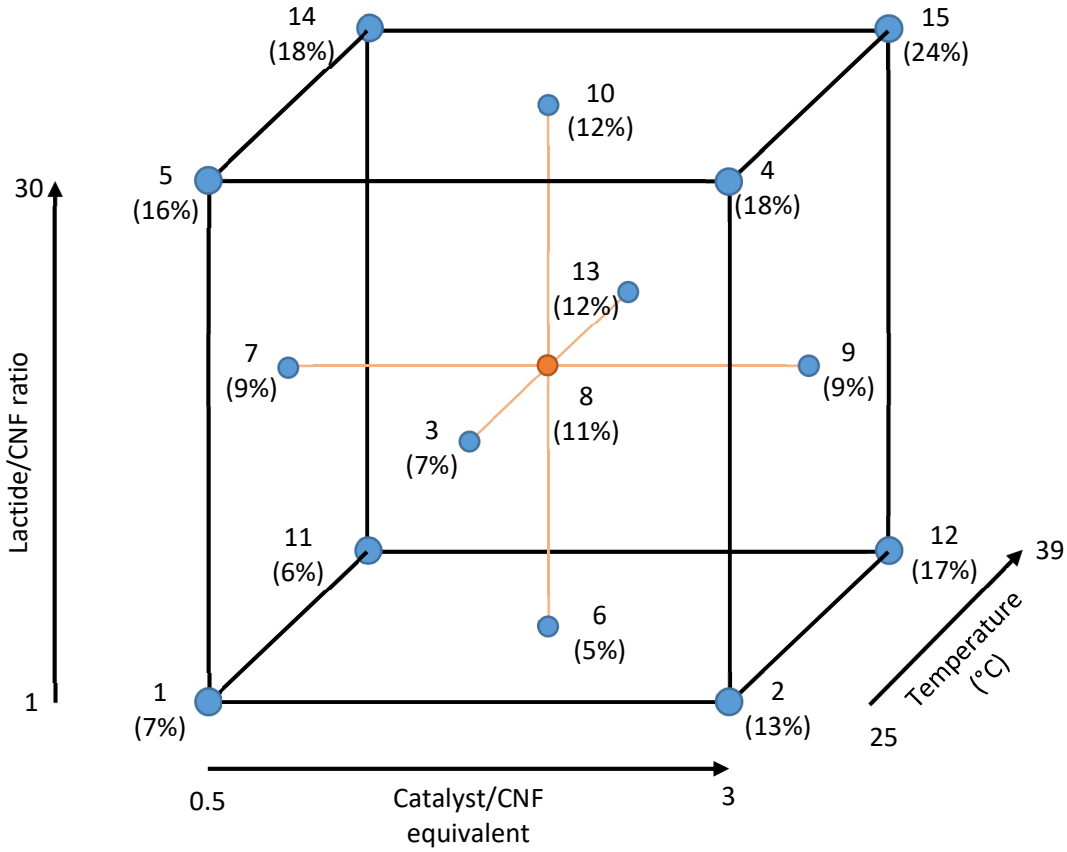

Figure 4: graphical representation of the grafting % of PLA on cellulose with different sets of parameters. Numbers correspond to entries in table 2

At higher temperatures but low monomer amount (entry 11 and 12), the increase in DMAP content has more of an impact on the amount of PLA grafted which increased by 11%, compared to a 5% increase at lower temperature. This is likely due to a faster polymerization of lactide at higher temperatures, but initiation being preferred for water as it is more mobile and available than cellulose OH groups, resulting in homopolymerization being heavily favored. An opposite effect is observed at lower temperatures and a high lactide amount (entry 5 and 4): An increase in the quantity of DMAP did not make a noticeable difference in the surface-grafted quantity of PLA (2%). If polymerization on cellulose "starts late" due to

initiation on water being faster, but there is a lot more monomer available and propagation is slower, then grafting on cellulose still has time to occure. In that regard, adding more DMAP to ensure initiation on cellulose can happen quickly does increase the amount of grafting found, but only by a small margin.

An increase in temperature (entry 1 to 11, 2 to 12, 5 to 14 and 4 to 15) in general led to a greater amount of grafted PLA on the CNF, similarly to an increase in catalyst amount. However this effect was more pronounced for higher catalyst amounts, as increasing the temperature from 25 to 39°C when only 0.5 eq of DMAP was used (entry 1 *vs.* 11, 2 *vs.* 12, 5 *vs.* 14 and 4 *vs.* 15) did not make a significant difference (2% or less) in the amount of PLA grafted on the CNFs, irrespective of amount of monomer. While increasing the temperature was beneficial to the amount of PLA grafting, it may also lead to faster polymerization, while the lower amount of catalyst may lead to a slower initiation on CNF surface hydroxyl, both of which favor water-initiated homopolymerization.

Finally, the effect of the monomer quantity was studied. When comparing the results of entry 1 *vs.* 5, 2 *vs.* 4, 11 *vs.* 14, 12 *vs.* 15 and 6 *vs.* 10, the PLA weight content on modified CNF increased significantly with increasing amounts of lactide. This particular effect was more pronounced for a smaller quantity of catalyst, leading to an increase of 9% (entry 1 to 5) and 12% (entry 11 to 14) in PLA grafting. Comparatively, increasing the monomer amount at higher DMAP loading increased the PLA amount on CNF by 5% (entry 2 to 4) and 7% (entry 12 to15) respectively. This result agrees with the previous observations, showing that a small amount of catalyst favors initiation by residual water, which then will quickly turn the monomer into homopolymer. When more lactide is added to the reaction, this effect is mitigated as more monomer takes longer to react away allowing for surface-grafting on the nanocellulose.

Comparing all reactions, the monomer amount comes out as the most influential parameter, as an increase in *rac*-lactide always led to the most significant increase in grafting amount on CNF. However, increasing the amount of catalysts can achieve comparable results, especially at higher temperatures. This can be more advantageous as the amount of catalyst needed to yield such result is significantly less than the amount of monomer required, as an increase by a factor 6 for the quantity of catalysts can yield similar amount of grafting as an increase by a factor 30 for the quantity of monomer.

Reactions with intermediate values for all parameters were also performed to verify the trends. While those observations stayed true for most experiments, some specific combinations gave low PLA grafting onto cellulose, meaning some parameter combinations do not favor grafting, but rather water-initiated homopolymerization. In particular, increasing the temperature was detrimental to PLA grafting on CNF for low DMAP and lactide quantities, explained by the temperature increasing the speed of homopolymerization.

Compared to the results for freeze-dried CNF, solvent-exchanging CNF allows for a higher maximum grafting efficiency, but significantly better results are obtained for reactions performed with less than 3 eq of catalysts, all the while requiring shorter reaction times. In addition, elemental analysis showed no

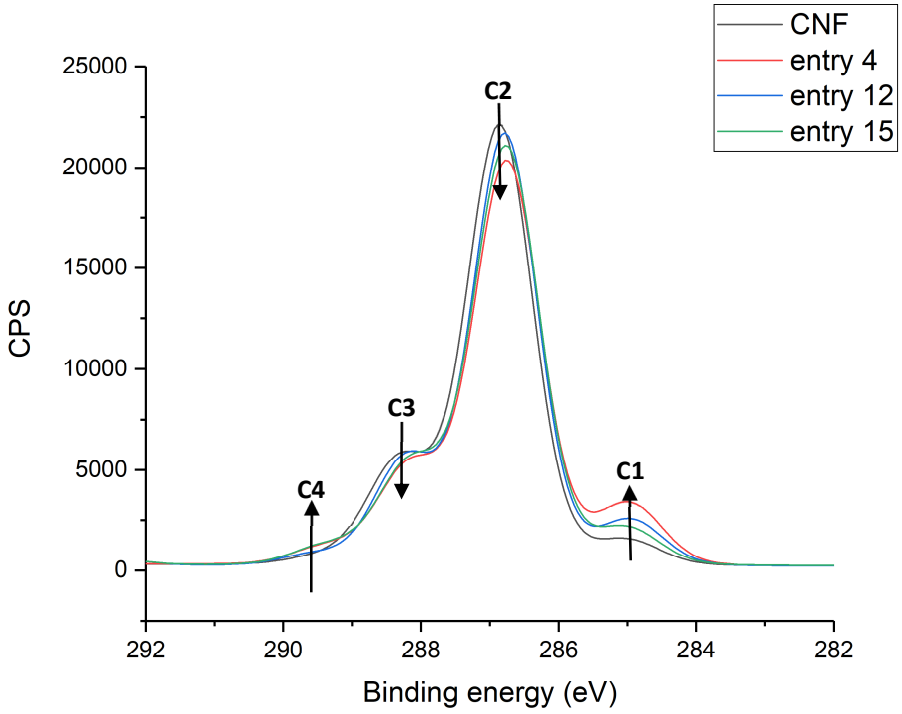

Figure 5: Carbon 1s XPS scan of modified cellulose nanofibrils (CNF) obtained from dispersion in dichloromethane, with different entries corresponding to the samples in Table 2

significant retention of DMAP in the grafted CNF, indicating a near complete removal of the catalyst from the product. FT-IR (Supporting Information Section 2) analysis showed a band around 1750 cm^{-1}, characteristic of a stretching frequency for ν(C=O). A characteristic ester band is seen at 1454 cm^{-1} and is more important for the cellulose with a higher PLA content. As shown in the magnification the carbonyl signal increase, following the same trend as the amount of grafting calculated using EA. Comparing the spectra obtained using the freeze-dried CNF, the overall signal is similar, and the relative intensity of the ester band is similar for samples with equal PLA content calculated with EA.

X-ray photoelectron spectroscopy (Figure 5), shows the aliphatic carbon contribution C1 increasing for modified CNF compared to non-modified ones due to the methyl-bearing lactide units grafted on the cellulose. The same conclusion can be made for the C4 contribution, related to O-C=O visible at 289.54 eV present only on the grafts.

When comparing the XPS results for the never dried CNF to the one in Figure 3, the same peaks can be seen. However, increases are more pronounced for samples prepared with freeze-dried cellulose, despite

EA showing higher grafting for never-dried CNF. A plausible explanation could be that XPS is a surface analysis, only revealing the composition of the top 10 nm of the material. Freeze-dried CNF is more aggregated in the reaction mixture and in the final product. The majority of grafting will thus occur on the surface of aggregated CNF particles, leading to a stronger signal in XPS, yet a lower EA amount. The well-dispersed CNF form a powdery product however, and it is likely that the better dispersion leads to a better separation of the fibrils, giving more surface area for the graft to occur, thus graft may be present deeper in the material.

To confirm that lactide polymerization did indeed occur during the reaction and determine the potential length of the PLA chains obtained, size-exclusion chromatography (SEC) was used to determine the length of the homopolymer separated from the CNF during the soxhlet extraction. Overall, the results showed that short oligomer chains were obtained, with a number average molecular weight between 600 and 1400 g/mol, confirming the successful polymerization reaction and the presence of chains initiated by water.

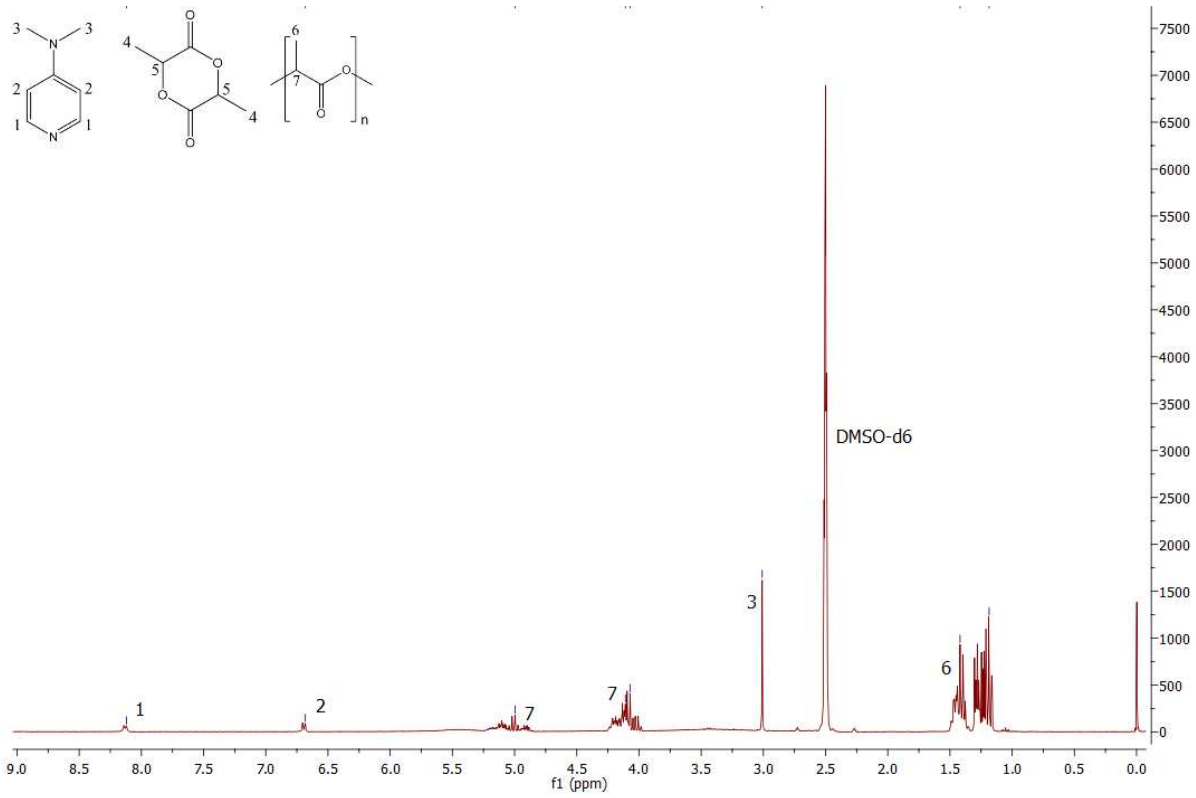

Figure 6: 1H NMR spectra of crude mixture after reaction in DMSO-d6. Crude product separated from modified CNF corresponding to entry 15 in table 2

As a complementary approach to determine polymerization of lactide, NMR was used on some crudes samples separated from CNF, similar to the one used for SEC analysis. Samples separated from CNF with

different % of grafting (according to EA) were analyzed and compared to the spectra of DL-Lactide and DMAP.

^{1}H NMR (DMSO-d6, 300 MHz) δ (ppm) 8.16 (s, 2H), 6.72 (s, 2H), 4.86-5.21 (m, 1H), 4.10-4.24 (m, 1H), 3.01 (s, 6H), 1.16-1.49 (m, 3H)

Characteristic doublet are observed at 8.16 and 6.72 ppm, corresponding to protons on the pyridine ring of DMAP. Additionally, a singlet corresponding to CH_3 moieties of DMAP is also observed at 3.01 ppm. As the analysis was performed on crude product separated from cellulose, the presence of catalyst was expected.

Complex signals can be observed between in the region 4.86-5.21 ppm and 4.10-4.24 ppm. This corresponds to the proton in the polymerized lactide chain. Protons closer to chain ends have a different chemical shift, which leads to 2 complex multiplet. Due to the short length of the oligomer produced, protons next to chain ends have a strong signal in NMR.

A similar phenomenon can be observed between 1.16 and 1.49 ppm, which corresponds to methyl protons.

Interestingly, the signal for lactide in DMSO, particularly for the proton in the 6 membered ring, is not observed around 5.43 ppm where a quartet should be in the presence of DL-Lactide. This shows that while the grafting measured on CNF is low, and only short oligomers are produced, the conversion of monomer does occur.

Overall using never-dried CNF with DMAP and *rac*-lactide has been the more promising grafting method. While both method used for never-dried and freeze-dried CNF are different, and a quantitative comparison cannot be done, the second method used shows more promising results, in particular when trying to use lower quantities of catalyst. It also does not require freeze-drying, a method than can at times take several days, and leads to a better dispersed state of cellulose which is overall easier to analyses.

4. Conclusion

We performed SI-ROP of *rac*-lactide using an organocatalyst, N,N-dimethyl aminopyridine (DMAP), and CNFs as the initiator. The effect of different parameters on the reaction were investigated as well as the interaction between these parameters on the modification of cellulose. The highest modification amount was achieved for never-dried CNF suspensions transferred into DCM by solvent exchange, as opposed to the more common lyophilization procedure. The highest grafting was obtained for a 3/1 ratio of

382 DMAP/CNF, 3 g of *rac*-lactide, a reaction time of 24 h at 39°C under inert atmosphere. The amount of
383 modification was similar to earlier reports using tin(II) octoate as the catalyst in solution at 90°C or in bulk
384 at 120°C (Stepanova et al. 2019), while we used a simple one-step reaction and an organic catalyst under
385 mild conditions. In addition, most of the catalyst could be removed from the final product. We were also
386 able to elucidate the effect of changing parameters on the effect of residual water interference of the grafting
387 reaction.

388

389 ## 5. Acknowledgement

390 The authors are grateful to Aurélie Malfait for SEC measurements. The authors also acknowledge
391 financial support from the Initiatives for Science, Innovation, Territories and Economy (I-SITE) Lille
392 Nord – Europe, from Research Foundation Flanders (grant G0C6013N), KU Leuven (grant C14/18/061)
393 and from the European Union's European Fund for Regional Development, Flanders Innovation &
394 Entrepreneurship, and the Province of West-Flanders for financial support in the Accelerate^3 project
395 (Interreg Vlaanderen-Nederland program).

396

6. References:

Abitbol, T., Kloser, E., & Gray, D. G. (2013). Estimation of the surface sulfur content of cellulose nanocrystals prepared by sulfuric acid hydrolysis. *Cellulose*, *20*(2), 785–794.

Avinc, O., & Khoddami, A. (2009). Overview of Poly(Lactic Acid) (PLA). *Fiber chemistry, vol 41, No.6*

Bondeson, D., & Oksman, K. (2007). Dispersion and characteristics of surfactant modified cellulose whiskers nanocomposites. *Composite Interfaces*, *14*(7–9), 617–630.

Bondeson, D., Mathew, A., & Oksman, K. (2006). Optimization of the isolation of nanocrystals from microcrystalline cellulose by acid hydrolysis. *Cellulose*, *13*(2), 171–180.

de Nooy, A. E. J., Besemer, A. C., & van Bekkum, H. (2010). Highly selective tempo mediated oxidation of primary alcohol groups in polysaccharides. *Recueil Des Travaux Chimiques Des Pays-Bas*, *113*(3), 165–166.

Dove, A. P. (2012). Organic Catalysis for Ring-Opening Polymerization. *ACS Macro Letters*, *1*(12), 1409–1412.

Drumright, R. E., Gruber, P. R., & Henton, D. E. (2000). *Polylactic Acid Technology*. 6.

Dufresne, A. (2013). Nanocellulose: a new ageless bionanomaterial. *Materials Today*, *16*(6), 220–227.

Eichhorn, S. J., Dufresne, A., Aranguren, M., Marcovich, N. E., Capadona, J. R., Rowan, S. J., Weder, C., Thielemans, W., Roman, M., Renneckar, S., Gindl, W., Veigel, S., Keckes, J., Yano, H., Abe, K., Nogi, M., Nakagaito, A. N., Mangalam, A., Simonsen, J., … Peijs, T. (2010). Review: current international research into cellulose nanofibres and nanocomposites. *Journal of Materials Science*, *45*(1), 1–33.

Eyley, S., & Thielemans, W. (2014). Surface modification of cellulose nanocrystals. *Nanoscale*, *6*(14), 7764–7779.

Eyley, S., Schütz, C., & Thielemans, W. (2018). Surface Chemistry and Characterization of Cellulose Nanocrystals. In T. Rosenau, A. Potthast, & J. Hell (Eds.), *Cellulose Science and Technology* (pp. 223–252). John Wiley & Sons, Inc.

Gazzotti, S., Rampazzo, R., Hakkarainen, M., Bussini, D., Ortenzi, M. A., Farina, H., Lesma, G., & Silvani, A. (2019). Cellulose nanofibrils as reinforcing agents for PLA-based nanocomposites: An in situ approach. *Composites Science and Technology*, *171*, 94–102.

425 Goussé, C., Chanzy, H., Excoffier, G., Soubeyrand, L., & Fleury, E. (2002). Stable suspensions of
426 partially silylated cellulose whiskers dispersed in organic solvents. *Polymer*, *43*(9), 2645–2651.

427 Habibi, Y. (2014). Key advances in the chemical modification of nanocelluloses. *Chem. Soc. Rev.*, *43*(5),
428 1519–1542.

429 Habibi, Y., Lucia, L. A., & Rojas, O. J. (2010). Cellulose Nanocrystals: Chemistry, Self-Assembly, and
430 Applications. *Chemical Reviews*, *110*(6), 3479–3500.

431 Hafrén, J., & Córdova, A. (2005). Direct Organocatalytic Polymerization from Cellulose Fibers: Direct
432 Organocatalytic Polymerization from Cellulose Fibers. *Macromolecular Rapid Communications*,
433 *26*(2), 82–86.

434 Hasani, M., Cranston, E. D., Westman, G., & Gray, D. G. (2008). Cationic surface functionalization of
435 cellulose nanocrystals. *Soft Matter*, *4*(11), 2238–2244.

436 Heux, L., Chauve, G., & Bonini, C. (2000). Nonflocculating and Chiral-Nematic Self-ordering of
437 Cellulose Microcrystals Suspensions in Nonpolar Solvents. *Langmuir*, *16*(21), 8210–8212.

438 Isogai, A., Saito, T., & Fukuzumi, H. (2011). TEMPO-oxidized cellulose nanofibers. *Nanoscale*, *3*(1),
439 71–85.

440 Kiesewetter, M. K., Shin, E. J., Hedrick, J. L., & Waymouth, R. M. (2010). Organocatalysis:
441 Opportunities and Challenges for Polymer Synthesis. *Macromolecules*, *43*(5), 2093–2107.

442 Labet, M. (2012). Grafting *ε-Caprolactone from the Surface of Polysaccharide Nanocrystals:* PhD
443 Thesis, The University of Nottingham, p. 258.

444 Labet, M., & Thielemans, W. (2011). Improving the reproducibility of chemical reactions on the surface
445 of cellulose nanocrystals: ROP of ε-caprolactone as a case study. *Cellulose*, *18*(3), 607–617.

446 Labet, M., & Thielemans, W. (2012). Citric acid as a benign alternative to metal catalysts for the
447 production of cellulose-grafted-polycaprolactone copolymers. *Polymer Chemistry*, *3*(3), 679.

448 Labet, M., Thielemans, W., & Dufresne, A. (2007). Polymer Grafting onto Starch Nanocrystals.
449 *Biomacromolecules*, *8*(9), 2916–2927.

450 Lasseuguette, E. (2008). Grafting onto microfibrils of native cellulose. *Cellulose*, *15*(4), 571–580.

451 Li, H., Ai, B.-R., & Hong, M. (2018). Stereoselective ring-opening polymerization of rac-lactide by bulky
452 chiral and achiral N-heterocyclic carbenes. *Chinese Journal of Polymer Science*, *36*(2), 231–236.

Liimatainen, H., Visanko, M., Sirviö, J., Hormi, O., & Niinimäki, J. (2013). Sulfonated cellulose nanofibrils obtained from wood pulp through regioselective oxidative bisulfite pre-treatment. *Cellulose*, *20*(2), 741–749.

Liu, J.-C., Moon, R. J., Rudie, A., & Youngblood, J. P. (2014). Mechanical performance of cellulose nanofibril film-wood flake laminate. *Holzforschung*, *68*(3), 283–290.

Lohmeijer, B. G. G., Pratt, R. C., Leibfarth, F., Logan, J. W., Long, D. A., Dove, A. P., Nederberg, F., Choi, J., Wade, C., Waymouth, R. M., & Hedrick, J. L. (2006). Guanidine and Amidine Organocatalysts for Ring-Opening Polymerization of Cyclic Esters. *Macromolecules*, *39*(25), 8574–8583.

Miao, Y., Rousseau, C., Mortreux, A., Martin, P., & Zinck, P. (2011). Access to new carbohydrate-functionalized polylactides via organocatalyzed ring-opening polymerization. *Polymer*, *52*(22), 5018–5026.

Munim, S. A., & Raza, Z. A. (2019). Poly(lactic acid) based hydrogels: formation, characteristics and biomedical applications. *Journal of Porous Materials*, *26*(3), 881–901.

Nederberg, F., Connor, E. F., Möller, M., Glauser, T., & Hedrick, J. L. (2001). New Paradigms for Organic Catalysts: The First Organocatalytic Living Polymerization. *Angewandte Chemie International Edition 40, No. 14*, 2712-2715

Nogueira, G., Favrelle, A., Bria, M., Prates Ramalho, J. P., Mendes, P. J., Valente, A., & Zinck, P. (2016). Adenine as an organocatalyst for the ring-opening polymerization of lactide: scope, mechanism and access to adenine-functionalized polylactide. *Reaction Chemistry & Engineering*, *1*(5), 508–520.

Nordgren, N., Lönnberg, H., Hult, A., Malmström, E., & Rutland, M. W. (2009). Adhesion Dynamics for Cellulose Nanocomposites. *ACS Applied Materials & Interfaces*, *1*(10), 2098–2103.

Ohkita, T., & Lee, S.-H. (2004). Effect of aliphatic isocyanates (HDI and LDI) as coupling agents on the properties of eco-composites from biodegradable polymers and corn starch. *Journal of Adhesion Science and Technology*, *18*(8), 905–924.

Ottou, W. N., Sardon, H., Mecerreyes, D., Vignolle, J., & Taton, D. (2016). Update and challenges in organo-mediated polymerization reactions. *Progress in Polymer Science*, *56*, 64–115.

Ouchi, T., Kontani, T., & Ohya, Y. (2003). Modification of polylactide upon physical properties by solution-cast blends from polylactide and polylactide-grafted dextran. *Polymer*, *44*(14), 3927–3933.

Simón, L., & Goodman, J. M. (2007). The Mechanism of TBD-Catalyzed Ring-Opening Polymerization of Cyclic Esters. *The Journal of Organic Chemistry*, *72*(25), 9656–9662.

Siqueira, G., Bras, J., & Dufresne, A. (2010). Cellulosic Bionanocomposites: A Review of Preparation, Properties and Applications. *Polymers*, *2*(4), 728–765.

Stepanova, M., Averianov, I., Gofman, I., Solomahka, O., Nashchekina, Y., Korzhikov-Vlakh, V., Korzhikov-Vlakh, E. (2019). Poly(ε-caprolactone)-based biocomposites reinforced with nanocrystalline cellulose grafted with poly(L-lactic acid), *IOP Conf. Series: Materials Science and Engineering 500*, 01021.

Trache, D., Hussin, M. H., Haafiz, M. K. M., & Thakur, V. K. (2017). Recent progress in cellulose nanocrystals: sources and production. *Nanoscale*, *9*(5), 1763–1786.

Xie, H., Du, H., Yang, X., & Si, C. (2018). Recent Strategies in Preparation of Cellulose Nanocrystals and Cellulose Nanofibrils Derived from Raw Cellulose Materials. *International Journal of Polymer Science*, *2018*, 1–25.

Xu, X., Liu, F., Jiang, L., Zhu, J. Y., Haagenson, D., & Wiesenborn, D. P. (2013). Cellulose Nanocrystals vs. Cellulose Nanofibrils: A Comparative Study on Their Microstructures and Effects as Polymer Reinforcing Agents. *ACS Applied Materials & Interfaces*, *5*(8), 2999–3009.

Yamamoto, H., Horii, F., & Hirai, A. (2006). Structural studies of bacterial cellulose through the solid-phase nitration and acetylation by CP/MAS 13C NMR spectroscopy. *Cellulose*, *13*(3), 327–342.

Yang, Z.-Y., Wang, W.-J., Shao, Z.-Q., Zhu, H.-D., Li, Y.-H., & Wang, F.-J. (2013). The transparency and mechanical properties of cellulose acetate nanocomposites using cellulose nanowhiskers as fillers. *Cellulose*, *20*(1), 159–168.

Zhao, G., Du, J., Chen, W., Pan, M., & Chen, D. (2019). Preparation and thermostability of cellulose nanocrystals and nanofibrils from two sources of biomass: rice straw and poplar wood. *Cellulose*.